Odd-Time Reversal $\mathcal{PT}$ Symmetry Induced by an Anti-$\mathcal{PT}$-Symmetric Medium

Vladimir V. Konotop[1] and Dmitry A. Zezyulin[2]
[1]Departamento de Física and Centro de Física Teórica e Computacional, Faculdade de Ciências, Universidade de Lisboa, Campo Grande 2, Edifício C8, Lisboa 1749-016, Portugal
[2]ITMO University, St. Petersburg 197101, Russia

(Received 11 December 2017; published 22 March 2018)

We introduce an optical system (a coupler) obeying parity-time ($\mathcal{PT}$) symmetry with odd-time reversal, $\mathcal{T}^2 = -1$. It is implemented with two birefringent waveguides embedded in an anti-$\mathcal{PT}$-symmetric medium. The system possesses properties that are untypical for most physical systems with the conventional even-time reversal. Having a symmetry-protected degeneracy of the linear modes, the coupler allows for the realization of a coherent switch operating with a superposition of binary states that are distinguished by their polarizations. When a Kerr nonlinearity is taken into account, each linear state, being doubly degenerated, bifurcates into several distinct nonlinear modes, some of which are dynamically stable. The nonlinear modes are characterized by amplitude and by polarization and come in $\mathcal{PT}$-conjugate pairs.

DOI: 10.1103/PhysRevLett.120.123902

Introduction.—The concepts of parity $\mathcal{P}$ and time $\mathcal{T}$ symmetries, intensively discussed in the context of non-Hermitian quantum mechanics since the seminal work [1], has nowadays acquired great significance in practically all areas of physics dealing with linear and nonlinear wave phenomena [2]. The universality of the paradigm, first recognized in optics [3–5], is based on the mathematical similarity between the parabolic equation describing light propagation in various settings and the Schrödinger equation governing the dynamics of a nonrelativistic quantum particle. Respectively, the parity and time inversion operators used in most of the applications had the same form as those for a spinless quantum particle, i.e., $\mathcal{P}\psi(\mathbf{r},t) = \psi(-\mathbf{r},t)$ and $\mathcal{T}\psi(\mathbf{r},t) = \psi^*(\mathbf{r},-t)$. From the theoretical point of view, however, the operators $\mathcal{P}$ and $\mathcal{T}$ can have a much more general form [6]. As a matter of fact, various definitions of the parity operator, which is an involution, i.e., satisfies $\mathcal{P}^2 = 1$, have already been explored in discrete optics. For instance, for dimer models the operator $\mathcal{P}$ is tantamount to the σ_1 Pauli matrix [4], and in more complex quadrimer and oligomer models $\mathcal{P}$ can be defined as the Kronecker products of Pauli matrices [2,7,8]. The time reversal operator $\mathcal{T}$ is antilinear and, in quantum mechanics, it is even for bosons, $\mathcal{T}^2 = 1$, and odd for fermions, $\mathcal{T}^2 = -1$ [9]. However, only the former possibility was used in all classical applications (i.e., beyond quantum mechanics) of the non-Hermitian physics.

Non-Hermitian quantum mechanics with odd time reversal, $\mathcal{T}^2 = -1$, has been brought to the discussion by a series of works initiated by Refs. [10,11]. The respective Hamiltonians display interesting properties (some of them are recalled below) that, however, have never been explored in other physical applications. This leads to the first goal of this Letter, which is to introduce an optical system obeying odd $\mathcal{PT}$ symmetry. We illustrate the utility of such a system with two examples. First, we propose a coherent optical switch that operates with linear superpositions of binary states, rather than with single states, as the conventional switches based on even $\mathcal{PT}$ symmetry do [12]. Second, we describe peculiarities of nonlinear modes in odd-$\mathcal{PT}$ systems, where the nonlinearity is odd-$\mathcal{PT}$ symmetric, too.

Let us also recall other recent developments in optics of media with special symmetries. It was suggested in Ref. [13] to explore properties of anti-$\mathcal{PT}$-symmetric optical media that are characterized by dielectric permittivities with $\varepsilon(\mathbf{r}) = -\varepsilon^*(-\mathbf{r})$ and can be realized, say, in metamaterials. More recently, the experimental realization of anti-$\mathcal{PT}$-symmetric media in atomic vapors has been reported in Ref. [14], and other schemes implementing the idea with dissipatively coupled optical systems have been designed in Ref. [15]. Practical applications of such media, however, remain unexplored. Thus, the second goal of this Letter is to show that an anti-$\mathcal{PT}$-symmetric medium is a natural physical environment where the odd $\mathcal{PT}$ symmetry can be realized.

Optical coupler with odd $\mathcal{PT}$ symmetry.—Consider a system of two birefringent waveguides, each one with orthogonal principal axes. To simplify the model, we neglect a mismatch between propagation constants of the polarizations inside each waveguide, but take into account a mismatch 2δ between the propagation constants of the waveguides: $q_{1,2} = q \mp \delta$, where q is the average propagation constant. Let these waveguides be coupled to each other by an isotropic medium with active and absorbing domains as schematically shown in Fig. 1. The components of the guided monochromatic electric fields can be written as $\mathbf{E}_1 = [\mathbf{e}_1 A_1(z)\psi_1(\mathbf{r}) + \mathbf{e}_2 A_2(z)\psi_2(\mathbf{r})]e^{i(q-\delta)z}$ and

$\mathbf{E}_2 = [\mathbf{e}_3 A_3(z)\psi_3(\mathbf{r}) + \mathbf{e}_4 A_4(z)\psi_4(\mathbf{r})]e^{i(q+\delta)z}$, where $\mathbf{r} = (x, y)$, $\mathbf{e}_j$ and $\psi_j(\mathbf{r})$ are the polarization vectors, and the respective transverse distributions of the modes, $A_j(z)$, are slowly varying field amplitudes that depend on the propagation distance z. The polarization axes in each waveguide are orthogonal, $\mathbf{e}_1\mathbf{e}_2 = \mathbf{e}_3\mathbf{e}_4 = 0$, and in different waveguides are mutually rotated by an angle α, ensuring the relations $\mathbf{e}_1\mathbf{e}_3 = \mathbf{e}_2\mathbf{e}_4 = \cos\alpha$ and $\mathbf{e}_1\mathbf{e}_4 = -\mathbf{e}_2\mathbf{e}_3 = -\sin\alpha$. The modes are weakly guided, so that the same polarization properties hold for the fields outside the waveguide cores.

Since $\mathbf{e}_1$ is orthogonal to $\mathbf{e}_2$ and $\mathbf{e}_3$ is orthogonal to $\mathbf{e}_4$, the coupling is possible only between one polarization in a given waveguide and two polarizations in another one. Such a coupling is determined by the overlapping integrals $\kappa_{jk} = \mathbf{e}_j\mathbf{e}_k \int \psi_j^*(\mathbf{r})\varepsilon(\mathbf{r})\psi_k(\mathbf{r})d^2\mathbf{r}$, where $j, k = 1, \ldots, 4$.

Let the medium in which the waveguides are embedded be anti-$\mathcal{PT}$-symmetric: $\varepsilon(\mathbf{r}) = -\varepsilon^*(-\mathbf{r})$. Assuming that $\psi_j(\mathbf{r}) \approx \psi_j(|\mathbf{r}|)$, i.e., the transverse field distribution is approximately radial, one ensures that $\kappa_{jk} = -\kappa_{kj}^*$, where $j = 1, 2$ and $k = 3, 4$. To further simplify the model, we consider the transverse distributions to differ only by phase mismatches φ and ϑ, according to the relations $\psi_1(\mathbf{r})e^{i(\varphi+\vartheta)/2} = \psi_2(\mathbf{r})e^{i(\vartheta-\varphi)/2} \equiv \psi(\mathbf{r} + \mathbf{r}_0)$ and $\psi_3(\mathbf{r})e^{i(\varphi+\vartheta)/2} = \psi_4(\mathbf{r})e^{i(\vartheta-\varphi)/2} \equiv \psi(\mathbf{r} - \mathbf{r}_0)$, where $\pm\mathbf{r}_0$ are the coordinates of the core centers (see Fig. 1). Thus, for the coupling coefficients we have $\kappa_{13} = \kappa_{24} = i\kappa\cos\alpha$ and $\kappa_{14} = \kappa_{23}^* = -i\kappa e^{i\varphi}\sin\alpha$, where $\kappa = -i\int \psi^*(\mathbf{r} - \mathbf{r}_0)\varepsilon(\mathbf{r})\psi(\mathbf{r} + \mathbf{r}_0)d^2\mathbf{r}$ is real. If the waveguides possess Kerr nonlinearity, one can write the system describing the evolution of the slowly varying amplitudes $\mathbf{A} = (A_1, A_2, A_3, A_4)^T$ (T stands for transpose) in the matrix from [16]

$$i\dot{\mathbf{A}} = H_\delta\mathbf{A} - F(\mathbf{A})\mathbf{A}, \qquad H_\delta = \begin{pmatrix} \delta\sigma_0 & i\kappa C \\ i\kappa C^\dagger & -\delta\sigma_0 \end{pmatrix}. \tag{1}$$

Here, σ_0 is the 2×2 identity matrix, C is the coupling matrix,

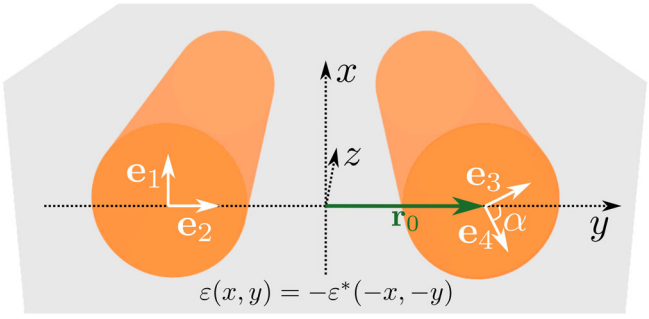

FIG. 1. Coupled transparent waveguides embedded in an anti-$\mathcal{PT}$-symmetric medium (see the text for notations).

$$C = \begin{pmatrix} e^{-i\vartheta}\cos\alpha & -e^{i\varphi}\sin\alpha \\ e^{-i\varphi}\sin\alpha & e^{i\vartheta}\cos\alpha \end{pmatrix}, \tag{2}$$

and the nonlinearity has the form known for birefringent waveguides [17]:

$$F(\mathbf{A}) = \mathrm{diag}\Big(|A_1|^2 + \frac{2}{3}|A_2|^2, |A_2|^2 + \frac{2}{3}|A_1|^2, |A_3|^2 + \frac{2}{3}|A_4|^2, |A_4|^2 + \frac{2}{3}|A_3|^2\Big). \tag{3}$$

The main feature of coupler (1), explored below, is that the coupling matrix C is a real quaternion [16]. Recalling the known results [10,11], one concludes that H_δ obeys odd $\mathcal{PT}$ symmetry with parity operator $\mathcal{P} = \gamma^0$, where γ^0 is the Dirac gamma matrix, and time reversal $\mathcal{T} = \sigma_0 \otimes (i\sigma_2)\mathcal{K}$, where $\mathcal{K}$ is the elementwise complex conjugation (note that $i\sigma_2\mathcal{K}$ is the usual time reversal operator for spin-1/2 fermions [9]). The relevant properties of the introduced operators are $\mathcal{P}^2 = 1$, $\mathcal{T}^2 = -1$, $[\mathcal{P}, \mathcal{T}] = 0$, and $[\mathcal{PT}, H_\delta] = 0$.

We start the analysis of system (1) with the linear limit, $F(\mathbf{A}) \equiv 0$. The guided modes are described by the eigenvalue problem $\tilde{b}\,\tilde{\mathbf{A}} = H_\delta\tilde{\mathbf{A}}$ (we use tildes for quantities that correspond to the linear limit). This problem is readily solved giving a pair of doubly degenerate eigenvalues, $\tilde{b}_\pm = \pm\sqrt{\delta^2 - \kappa^2}$, each having an invariant subspace spanned by two $\mathcal{PT}$-conjugate eigenvectors $\tilde{\mathbf{A}}_\pm^{(1)}$ and $\tilde{\mathbf{A}}_\pm^{(2)} = \mathcal{PT}\tilde{\mathbf{A}}_\pm^{(1)}$:

$$\tilde{\mathbf{A}}_\pm^{(1)} = \begin{pmatrix} \kappa e^{i\varphi}\sin\alpha \\ -\kappa e^{i\vartheta}\cos\alpha \\ 0 \\ i(\tilde{b}_\pm - \delta) \end{pmatrix}, \qquad \tilde{\mathbf{A}}_\pm^{(2)} = \begin{pmatrix} -\kappa e^{-i\vartheta}\cos\alpha \\ -\kappa e^{-i\varphi}\sin\alpha \\ i(\tilde{b}_\pm - \delta) \\ 0 \end{pmatrix}. \tag{4}$$

These vectors are mutually orthogonal: $\langle\tilde{\mathbf{A}}_\pm^{(1)}, \tilde{\mathbf{A}}_\pm^{(2)}\rangle = 0$, where $\langle\mathbf{A}, \mathbf{B}\rangle = \mathbf{A}^\dagger\mathbf{B}$ defines the inner product. For some general properties of odd-$\mathcal{PT}$-symmetric Hamiltonians see Ref. [10,11].

The odd $\mathcal{PT}$ symmetry does not exhaust all the symmetries of the system. In particular, the unitary transformation $\tilde{H} = SH_\delta S^{-1}$, where S is the block matrix defined as $S = \mathrm{diag}(e^{i(\vartheta-\varphi)\sigma_3/2}, e^{-i(\varphi+\vartheta)\sigma_3/2})$ results in an even-$\mathcal{PT}$-symmetric Hamiltonian $\tilde{H}$ with the same $\mathcal{P}$ operator and with conventional "bosonic" time reversal $\mathcal{K}$: $[\tilde{H}, \mathcal{PK}] = 0$. Additionally, H_δ anticommutes with the charge conjugation operator $\mathcal{C} = (\sigma_1 \otimes e^{i\sigma_3(\varphi-\pi/2)})\mathcal{K}$, this symmetry being responsible for the eigenvalues $\tilde{b}_\pm$ emerging in opposite pairs that are either real (unbroken phase, $|\kappa| < |\delta|$) or purely imaginary (broken phase, $|\kappa| > |\delta|$) [18].

Another important property of the odd $\mathcal{PT}$ symmetry is the existence of integrals of motion that can be found even in the nonlinear case. First, using that $\mathcal{P}H_\delta\mathcal{P} = H_\delta^\dagger$ and $\mathcal{P}F(\mathbf{A})\mathcal{P} = F^\dagger(\mathbf{A})$, one straightforwardly verifies [8] that $\mathcal{Q} = \mathbf{A}^\dagger\mathcal{P}\mathbf{A}$ is constant: $d\mathcal{Q}/dz = 0$. This conservation law locks the power imbalance in the waveguides: $\mathcal{Q} = P_1 - P_2 = \text{const}$, where $P_1 = |A_1|^2 + |A_2|^2$ and $P_2 = |A_3|^2 + |A_4|^2$. Furthermore, system (1) has a Hamiltonian structure. Indeed, defining a real-valued Hamiltonian $\mathcal{H} = \mathbf{A}^\dagger\mathcal{P}[H_\delta - F(\mathbf{A})/2]\mathbf{A}$ [16], Eq. (1) can be rewritten as $i\dot{A}_{1,2} = \partial\mathcal{H}/\partial A_{1,2}^*$ and $i\dot{A}_{3,4} = -\partial\mathcal{H}/\partial A_{3,4}^*$. Obviously, $\mathcal{H}$ is another conserved quantity: $d\mathcal{H}/dz = 0$.

Coherent switch.—Now we turn to examples illustrating features of the introduced coupler. Returning to the linear case, we observe that the double degeneracy of eigenstates is protected by the odd $\mathcal{PT}$ symmetry; i.e., the degeneracy cannot be lifted by any change of the parameters preserving $\mathcal{PT}$ symmetry. Thus, manipulating such a coupler, one simultaneously affects both the modes with the same propagation constant. This suggests an idea to perform a switching between a superposition of binary states, rather than between independent states as it happens with usual $\mathcal{PT}$-symmetric switches [12]. We call this device a coherent switch. Since the mentioned superposition can be characterized by a free parameter, such a system simulates a quantum switch for a superposition of states.

However, a solution for the coherent switch is not straightforward, because of the conservation of $\mathcal{Q}$, which means that an input signal, applied to only one waveguide, cannot be completely transferred to another one. Since this conservation is due to the $\mathcal{PT}$ symmetry, the complete energy transfer between the arms is possible only if the symmetry is broken by an additional element at some propagation interval. To this end, we explore the structure illustrated in Fig. 2: two couplers, with interchanged mismatches between the propagation constants, i.e., with $\delta \leftrightarrow -\delta$ in our notations, are connected by two decoupled waveguides. These auxiliary waveguides have balanced losses $-\Gamma$ and gain Γ, and have a mismatch between the propagation constants, denoted by $\pm\delta_0$. The lengths of the couplers are equal and chosen as $L = \pi/(2\sqrt{\delta^2 - \kappa^2})$ [we simplify the model letting $\vartheta = \varphi = 0$]. The decoupled segment, which disrupts the odd $\mathcal{PT}$ symmetry, has the length $\ell = \pi/(2\delta_0)$. The propagation in the couplers is governed by $H_{\pm\delta}$, and can be expressed through the evolution operators $U_{\pm\delta}(z, z+L) = -iH_{\pm\delta}/\sqrt{\delta^2 - \kappa^2}$ [16]. The evolution operator of the decoupled segment is diagonal: $U_0(z, z+\ell) = \text{diag}(ie^{-\Gamma\ell}, ie^{-\Gamma\ell}, -ie^{\Gamma\ell}, -ie^{\Gamma\ell})$. Thus, the output (at $z = 2L + \ell$) and input (at $z = 0$) fields are related by

$$\tilde{\mathbf{A}}_{\text{out}} = U_{-\delta}(L + \ell, 2L + \ell)U_0(L, L + \ell)U_\delta(0, L)\tilde{\mathbf{A}}_{\text{in}}. \tag{5}$$

The switch is controlled by the gain-and-loss coefficient Γ. Consider the situation when the input signal is applied to the first waveguide and has the polarization $\tilde{\mathbf{A}}_{\text{in}} = (\cos\chi, \sin\chi, 0, 0)^T$; i.e., $\tilde{\mathbf{A}}_{\text{in}}$ is parameterized by a free parameter χ (the red polarization vector at the input in Fig. 2). If the waveguides in the central part are conservative, $\Gamma = 0$, then the output signal is detected only at the first waveguide and arrives $\pi/2$ phase shifted: $\tilde{\mathbf{A}}_{\text{out}}^{(0)} = i\tilde{\mathbf{A}}_{\text{in}}$. If however $\Gamma = \Gamma_{\text{sw}} = \ell^{-1}\ln(\delta/\kappa)$, then the output signal has a polarization rotated by angle $-\alpha$ and is detected only in the second waveguide: $\tilde{\mathbf{A}}_{\text{out}} = (0, 0, \cos(\chi - \alpha), \sin(\chi - \alpha))^T$ (blue polarization vectors in Fig. 2). Importantly, χ, i.e., the ratio between the polarization components, remains a free parameter. The power distributions in the waveguides in the regime of switching are shown in the lower panel of Fig. 2. Inside the couplers, both $P_{1,2}$ grow or decay simultaneously. However, in the central segment with disrupted odd $\mathcal{PT}$ symmetry the powers are adjusted in such a way that the complete energy transfer is observed at the output.

Nonlinear modes.—As the second example illustrating the unconventional features of our system, we consider peculiarities of modes guided in a nonlinear coupler (1) with odd-time $\mathcal{PT}$ symmetry. Stationary solutions are searched in the form $\mathbf{A} = e^{-ibz}\mathbf{a}$, where b is a constant, and the amplitude vector $\mathbf{a}$ solves the algebraic system $b\mathbf{a} = H_\delta\mathbf{a} - F(\mathbf{a})\mathbf{a}$. Since the nonlinearity is $\mathcal{PT}$ symmetric [8], i.e., $[\mathcal{PT}, F(\mathbf{a})] = 0$, the nonlinear modes with the same propagation constant appear in $\mathcal{PT}$-conjugate pairs: $\mathbf{a}$ and $\mathcal{PT}\mathbf{a}$. Thus, the nonlinearity does not lift the degeneracy, and both $\mathcal{PT}$-conjugate modes are characterized by equal total powers $P = P_1 + P_2 = \mathbf{a}^\dagger\mathbf{a}$. The

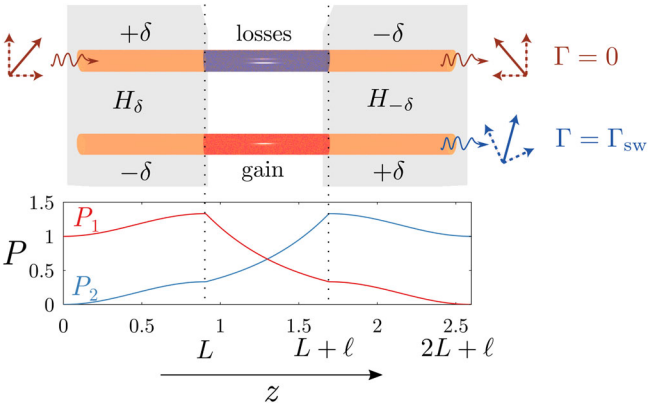

FIG. 2. The upper panel shows schematically the coherent switch. Shadowed domains correspond to anti-$\mathcal{PT}$-symmetric media. The central empty part illustrates the uncoupled waveguides with gain and losses. The polarization vectors at the output indicate (schematically) $\pi/2$-phase rotation of the nonswitched signal (at $\Gamma = 0$, red), and switching of the superposition rotated by angle $-\alpha$ (at $\Gamma = \Gamma_{\text{sw}}$, blue). The lower panel shows power distributions in the first P_1 (red line) and second P_2 (blue line) arms at Γ_{sw}, obtained for $\delta = \delta_0 = 2$ and $\kappa = 1$.

dependence $P(b)$ characterizes a family of modes; distinct families have different functional dependencies $P(b)$. Thus, any result for a family $P(b)$ discussed below applies to the pair of $\mathcal{PT}$-conjugate families.

We start by analyzing how the nonlinearity affects linear modes, i.e., with the weakly nonlinear case. It is known [7,19] that, in a system with an even $\mathcal{PT}$ symmetry without degeneracy of eigenstates, a linear eigenvalue bifurcates into a single family of nonlinear modes. But in a system with odd $\mathcal{PT}$ symmetry the situation can be more intricate, since the eigenvalues are degenerate, and one has to contemplate the effect of nonlinearity on a linear combination of independent eigenstates. The latter can be written as $\tilde{\mathbf{A}}_s = \sin(\nu)\tilde{\mathbf{A}}_s^{(1)} + \cos(\nu)e^{i\chi}\tilde{\mathbf{A}}_s^{(2)}$, where ν and χ are real parameters and s stands for either "+" or "−." Following Refs. [8,20], we look for a small-amplitude nonlinear mode in the form of expansions $b_s = \tilde{b}_s + \epsilon^2\beta_s + \cdots$, and $\mathbf{a}_s = \epsilon\tilde{\mathbf{A}}_s + \epsilon^3\mathbf{A}_s^{(3)} + \cdots$, where $\epsilon \ll 1$ is a formal small parameter. From the ϵ^3-order equation we compute [16] $\beta_s = -\langle F(\tilde{\mathbf{A}}_s)\tilde{\mathbf{A}}_s^*, \tilde{\mathbf{A}}_s^{(j)}\rangle / \langle \tilde{\mathbf{A}}_s^*, \tilde{\mathbf{A}}_s^{(j)}\rangle$, which must be satisfied for both $j = 1, 2$. Additionally, the coefficient β_s is required to be real. These three requirements form the bifurcation conditions defining the parameters ν and χ for which bifurcations of nonlinear modes are possible.

Let us analyze the simple case of $\vartheta = \varphi = 0$ and $\alpha \in (0, \pi/4)$ [$\alpha = 0$, $\pi/4$ correspond to a trivial solution of parallel polarizations in the coupler arms]. Using computer algebra, one finds that the bifurcation conditions can be satisfied for two values of χ. At $\chi = \pi/2$, nonlinear modes can bifurcate from the linear limit at $\nu_0 = \pi/4$. These modes, however, have been found unstable in the entire range of their existence. A more interesting case is realized when each $\tilde{b}_s$ gives birth to two stable families of nonlinear modes: these correspond to $\chi = 0$ and $\nu = \nu_s$ given by

$$2\tan\nu_s = c_s \pm \sqrt{c_s^2 + 4} + \sqrt{\left(c_s \pm \sqrt{c_s^2 + 4}\right)^2 + 4},$$

where $c_s = 8\delta\tilde{b}_s(\delta - \tilde{b}_s)^2/[\kappa^4\sin(4\alpha)] - 2\tan(2\alpha)$. Using this analytical result, we performed numerical continuation of stable nonlinear modes from the small-amplitude limit to arbitrarily large amplitudes. An example of the resulting diagram is shown in Fig. 3(a), where we present two power curves $P(b)$ bifurcating from each eigenvalue $\tilde{b}_+$ and $\tilde{b}_-$. Tracing the dynamical stability of the modes along the power curves, we have found that the families bifurcating from $\tilde{b}_-$ are stable in the entire explored range, while both families from $\tilde{b}_+$ are stable for small powers and lose stability at large amplitudes.

To compute the polarizations of the modes, we notice that the stable nonlinear modes $\mathbf{a}$ bifurcating from the linear limit are $\mathcal{PK}$ invariant, i.e., $\mathcal{PK}\mathbf{a} = \mathbf{a}$. In our case this means that entries $a_{1,2}$ are purely real, and $a_{3,4}$ are purely imaginary. Thus, one can construct real-valued polarization

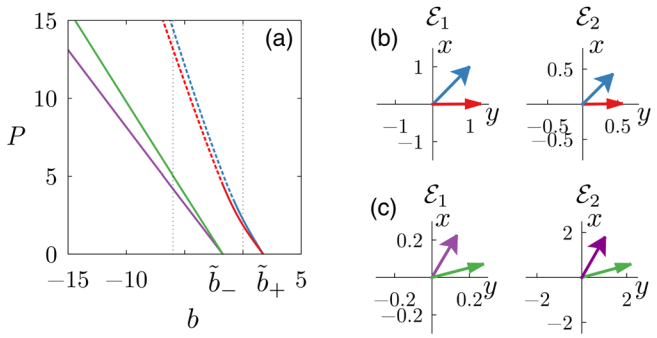

FIG. 3. (a) Families of solutions for $\delta = 2$, $\kappa = 1$, $\alpha = \pi/6$, $\vartheta = \varphi = 0$ visualized as dependencies P vs b. We show two families bifurcating from each eigenvalue $\tilde{b}_+$ and $\tilde{b}_-$. Stable and unstable modes are represented by solid and dotted segments, respectively. Vertical dotted lines indicate values $b = 0$ and $b = -6$ analyzed in (b) and (c) and Fig. 4. (b) Polarization vectors $\mathcal{E}_{1,2}$ in each waveguide for two stable nonlinear modes bifurcating from $\tilde{b}_+$, at $b = 0$. Arrows corresponding to the same mode have the same color as the respective family (and the same arrow head). (c) Polarization vectors $\mathcal{E}_{1,2}$ for two stable modes bifurcating from and $\tilde{b}_-$, at $b = -6$. The lengths of arrows $\mathcal{E}_{1,2}$ are equal to powers $P_{1,2}$ in each arm.

vectors $\mathcal{E}_1 = a_1\mathbf{e}_1 + a_2\mathbf{e}_2$ and $\mathcal{E}_2 = -ia_3\mathbf{e}_3 - ia_4\mathbf{e}_4$, where $\mathbf{e}_j$ are as defined above (see Fig. 1). Polarization vectors for several stable nonlinear modes are shown in Figs. 3(b) and 3(c). For each considered mode, polarizations $\mathcal{E}_1$ and $\mathcal{E}_2$ are nearly, but not exactly, parallel in both waveguides, and their direction varies slightly as the propagation constant changes. Thus, the main impact of the growing total power P is the increase of the moduli of $\mathcal{E}_1$ and $\mathcal{E}_2$. Figures 3(b) and 3(c) also explain the main difference between nonlinear modes bifurcating from $\tilde{b}_+$ and $\tilde{b}_-$. In the former (latter) case most of the total power is concentrated in the first (second) waveguide, i.e., $P_1 > P_2$ and $|\mathcal{E}_1| > |\mathcal{E}_2|$ ($P_2 > P_1$ and $|\mathcal{E}_2| > |\mathcal{E}_1|$).

Figure 4(a), where the dependencies P vs κ are plotted for a fixed propagation constant, illustrates the transformations of modes at the growing coupling strength κ. Four shown branches merge pairwise as κ increases (each

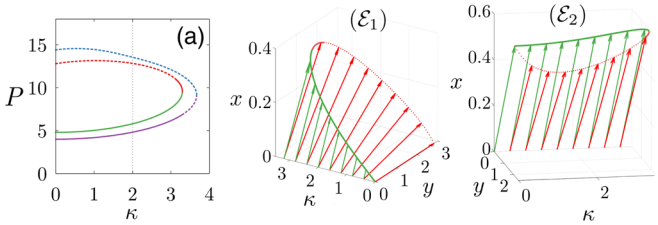

FIG. 4. (a) Branches of nonlinear modes for fixed $b = -6$, $\delta = 2$, and changing κ. Stable and unstable modes are represented by solid and dotted segments, respectively. The vertical dotted line indicates the $\mathcal{PT}$-symmetry-breaking threshold $\kappa = 2$. Panels $(\mathcal{E}_1)$ and $(\mathcal{E}_2)$ show polarization vectors corresponding to two merging branches (red and green curves) from (a).

solution bifurcating from the positive eigenvalue $\tilde{b}_+$ merges with some solution from $\tilde{b}_-$). Remarkably, the branches coalesce above the $\mathcal{PT}$-symmetry-breaking threshold $\kappa_{\mathcal{PT}} = \delta$ [which is equal to 2 in Fig. 3(b)]. Moreover, solutions can be stable above the $\mathcal{PT}$-symmetry-breaking point; in Figs. 3(a) and 3(b) stable modes are shown with solid lines. The polarization vectors of the nonlinear modes strongly depend on the coupling constant κ. This is illustrated in Figs. 4($\mathcal{E}_1$) and 4($\mathcal{E}_2$) where the heads of vectors $\mathcal{E}_{1,2}$ describe 3D curves in the (κ, x, y) space.

To conclude, we have introduced a $\mathcal{PT}$-symmetric optical coupler with odd-time reversal. The system features properties of an anti-$\mathcal{PT}$-symmetric medium in which two birefringent waveguides are embedded. As examples of applications, we described a coherent switch that operates with a linear superposition of binary states with one free parameter. As the second example, we report on bifurcations of families of nonlinear modes. An unusual observation was that each linear eigenstate gives rise to several distinct nonlinear modes, some of which are stable. Although we dealt with an optical model, the architecture of $\mathcal{PT}$-symmetric systems is generic and can be implemented in other physical systems.

The research of D. A. Z. is supported by Megagrant No. 14.Y26.31.0015 of the Ministry of Education and Science of Russian Federation.

[1] C. M. Bender and S. Boettcher, Real Spectra in Non-Hermitian Hamiltonians Having $\mathcal{PT}$-Symmetry, Phys. Rev. Lett. **80**, 5243 (1998); C. M. Bender, Making sense of non-Hermitian Hamiltonians, Rep. Prog. Phys. **70**, 947 (2007).

[2] V. V. Konotop, J. Yang, and D. A. Zezyulin, Nonlinear waves in $\mathcal{PT}$-symmetric systems, Rev. Mod. Phys. **88**, 035002 (2016).

[3] A. Ruschhaupt, F. Delgado, and J. G. Muga, Physical realization of $\mathcal{PT}$-symmetric potential scattering in a planar slab waveguide, J. Phys. A **38**, L171 (2005).

[4] R. El-Ganainy, K. G. Makris, D. N. Christodoulides, and Z. H. Musslimani, Theory of coupled optical PT-symmetric structures, Opt. Lett. **32**, 2632 (2007).

[5] Z. H. Musslimani, K. G. Makris, R. El-Ganainy, and D. N. Christodoulides, Optical Solitons in $\mathcal{PT}$ Periodic Potentials, Phys. Rev. Lett. **100**, 030402 (2008); K. G. Makris, R. El-Ganainy, D. N. Christodoulides, and Z. H. Musslimani, Beam Dynamics in $\mathcal{PT}$ Symmetric Optical Lattices, Phys. Rev. Lett. **100**, 103904 (2008).

[6] C. M. Bender, P. N. Meisinger, and Q. Wang, Finite-dimensional $\mathcal{PT}$-symmetric Hamiltonians, J. Phys. A **36**, 6791 (2003); A. Mostafazadeh, Exact $\mathcal{PT}$-symmetry is equivalent to Hermiticity, J. Phys. A **36**, 7081 (2003).

[7] K. Li and P. G. Kevrekidis, $\mathcal{PT}$-symmetric oligomers: Analytical solutions, linear stability, and nonlinear dynamics, Phys. Rev. E **83**, 066608 (2011); D. A. Zezyulin and V. V. Konotop, Nonlinear Modes in Finite-Dimensional $\mathcal{PT}$-Symmetric Systems, Phys. Rev. Lett. **108**, 213906 (2012); K. Li, P. G. Kevrekidis, B. A. Malomed, and U. Günther, Nonlinear $\mathcal{PT}$-symmetric plaquettes, J. Phys. A **45**, 444021 (2012).

[8] D. A. Zezyulin and V. V. Konotop, Stationary modes and integrals of motion in nonlinear lattices with a $\mathcal{PT}$-symmetric linear part, J. Phys. A **46**, 415301 (2013).

[9] A. Messiah, *Quantum Mechanics*, Vol. II (John Wiley & Sons, Inc., New York, 1966).

[10] K. Jones-Smith and H. Mathur, Non-Hermitian quantum Hamiltonians with PT symmetry, Phys. Rev. A **82**, 042101 (2010).

[11] C. M. Bender and S. P. Klevansky, $\mathcal{PT}$-symmetric representations of fermionic algebras, Phys. Rev. A **84**, 024102 (2011).

[12] F. Nazari, M. Nazari, and M. K. Moravvej-Farshi, A $\mathcal{PT}$ spatial optical switch based on $\mathcal{PT}$-symmetry, Opt. Lett. **36**, 4368 (2011); A. Lupu, H. Benisty, and A. Degiron, Switching using $\mathcal{PT}$-symmetry in plasmonic systems: Positive role of the losses, Opt. Express **21**, 21651 (2013); A. Lupu, H. Benisty, and A. Degiron, Using optical $\mathcal{PT}$-symmetry for switching applications, Photonics Nanostruct. Fundam. Appl. **12**, 305 (2014); A. Lupu, V. V. Konotop, and H. Benisty, Optimal $\mathcal{PT}$-symmetric switch features exceptional point, Sci. Rep. **7**, 13299 (2017).

[13] L. Ge and H. E. Türeci, Antisymmetric $\mathcal{PT}$-photonic structures with balanced positive-negative-index materials, Phys. Rev. A **88**, 053810 (2013).

[14] P. Peng, W. Cao, C. Shen, W. Qu, J. Wen, L. Jiang, and Y. Xiao, Anti-parity-time symmetry with flying atoms, Nat. Phys. **12**, 1139 (2016).

[15] F. Yang, Y.-C. Liu, and L. You, Anti-$\mathcal{PT}$ symmetry in dissipatively coupled optical systems, Phys. Rev. A **96**, 053845 (2017).

[16] See Supplemental Material at http://link.aps.org/supplemental/10.1103/PhysRevLett.120.123902 for some definitions, explicit presentations of some of the matrices, and comments on details of some of the algebra used in the main text.

[17] C. R. Menyuk, Nonlinear pulse propagation in birefringent optical fibers, IEEE J. Quantum Electron. **23**, 174 (1987).

[18] The existence of charge conjugation symmetry was noticed by the anonymous referee, who also pointed out that the Hamiltonian H_δ considered here belongs to class DIII of the classification introduced in S. Ryu, A. P. Schnyder, A. Furusaki, and A. W. W. Ludwig, Topological insulators and superconductors: tenfold way and dimensional hierarchy, New J. Phys. **12**, 065010 (2010).

[19] P. G. Kevrekidis, D. E. Pelinovsky, and D. Y. Tyugin, Nonlinear stationary states in PT-symmetric lattices, SIAM J. Appl. Dyn. Syst. **12**, 1210 (2013).

[20] K. Li, D. A. Zezyulin, V. V. Konotop, and P. G. Kevrekidis, Parity-time-symmetric optical coupler with birefringent arms, Phys. Rev. A **87**, 033812 (2013).